*32nd EPS Conference on Plasma Phys. Tarragona, 27 June - 1 July 2005 ECA Vol.**29C**, P-5.042 (2005)*

Confinement Scaling and Transport Properties in NSTX Plasmas

S.M. Kaye[1], M. G. Bell[1], R. E. Bell[1], E. D. Fredrickson[1], B. P. LeBlanc[1], K.C. Lee[2], S. A. Sabbagh[3], D. Stutman[4] and the NSTX Team

[1] *Princeton Plasma Physics Laboratory, Princeton University, Princeton, N.J. 08543*

[2] *University of California at Davis, Davis, Cal.*

[3] *Dept. of Applied Physics, Columbia Univ., NYC, N.Y.*

[4] *Johns Hopkins University, Baltimore, Md.*

Introduction

Data from neutral beam heating experiments in the low aspect ratio National Spherical Torus Experiment (NSTX) [1,2] greatly expands the range of data available for establishing both confinement and transport trends in toroidal confinement devices. For instance, the aspect ratio of NSTX is 1.3, a factor of two lower than those of conventional aspect ratio devices, and the NSTX data extend the range of toroidal beta from the conventional aspect ratio tokamak confinement database by a factor of 5, to values over 35%. Consequently, NSTX data provide a good test of conventional aspect ratio confinement scalings and transport trends, as well as an examination of the effects of extreme toroidicity, kinetic effects and high beta. The analysis to be presented in this paper is based on a dataset obtained during the 2004 experimental campaign in which R=0.83 to 0.89 m, a=0.57 to 0.66 m (R/a~1.3 to 1.45), I_p = 0.6 to 1.2 MA, B_T = 0.3 to 0.45 T, elongation κ = 1.7 to 2.4, triangularity δ=0.47 to 0.85 and n_e = 1.5 to 7.0 x 10^{19} m^{-3}. All discharges had deuterium neutral beam injection into deuterium plasmas, with P_{aux}=1.5 to 7 MW. Both L- and H-mode discharges were obtained during these experiments.

Global and Thermal Confinement

The confinement analysis to be presented here focuses on H-mode discharges. The set of H-mode discharges to be used were run primarily in the Lower Single Null configuration with the ion grad-B drift in the direction towards the X-point, to ensure the lowest L-H threshold powers ($\leq$1.5 MW) [3]. Dedicated scans were carried out in order to establish the scaling of confinement with both plasma current and heating power with other engineering parameters fixed. Fig. 1 shows the results of a scan in which the heating power was held fixed at approximately 4 MW, the elongation at 2.1 and the toroidal field at 0.45 T. The plasma current was varied in four steps from 0.6 to 1.2 MA. In this set of discharges, the total stored energy, as determined by EFIT [4], and the electron stored energy as determined from Thomson scattering measurements, both increase with increasing plasma current; at 0.5 s, their values scale nearly linearly with plasma current. There was a brief drop-out in the injected beam power for the 1.0 MA discharge, although this did not affect the ultimate stored energy attained. The same linear dependence of total and electron stored energy with plasma current was observed with injection powers of 6 MW. The density and temperature profiles taken near the time of peak electron stored energy (as denoted by the points on the respective time traces) are shown in the right-hand panels of the figure. The electron density varied by approximately 30% at these times over the range of currents, but the electron temperatures remained nearly constant. The "ears" on the density profile were caused by the buildup of carbon at the edge associated with the formation of an edge transport barrier during the early and mid H-mode phases. The ears tended to dissipate during the latter phase of the H-phase and during periods of strong ELM activity. Data from these dedicated scans and from discharges with similar operating parameters indicated that the global and thermal confinement times scaled nearly exactly linearly with I_p, although some of the increase in confinement may be due to the increasing density with I_p. The global and thermal

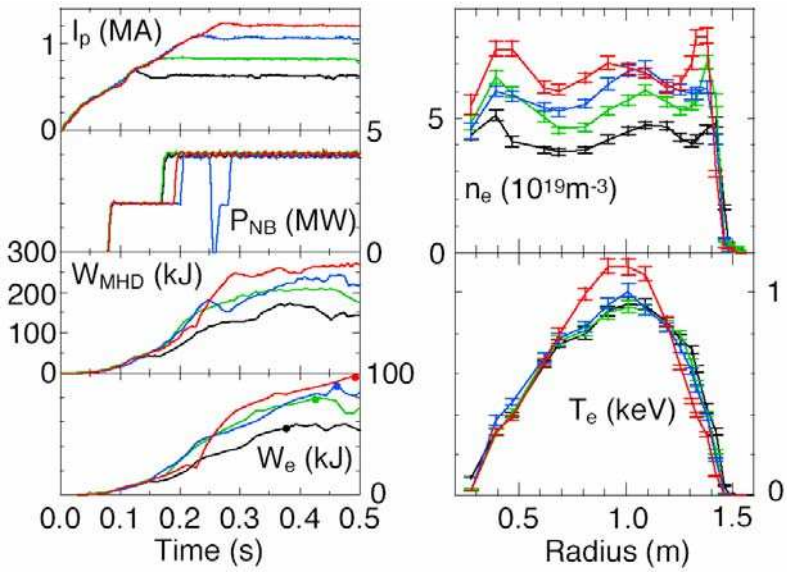

Fig. 1 Plasma and electron stored energy evolutions for discharges from a systematic current scaling experiment at fixed neutral beam power. Also shown are the electron temperature and density profiles for these discharges near the time of peak electron stored energy.

confinement times degraded with power as $P^{-0.40}$ and $P^{-0.57}$ respectively, a somewhat weaker degradation than observed at conventional aspect ratio [5].

The thermal confinement data, normalized to values given by the ITER98PBy,2 [5] scaling, are shown as a function of toroidal field in the left panel of Fig. 2. While the confinement data are consistent with the plasma current and power dependences exhibited at conventional aspect ratio, the left panel of Fig. 2 shows clearly that NSTX data exhibits a strong dependence on toroidal field. The figures show that the thermal τ_E values are enhanced over the L-mode value, with enhancement factors up to 1.4 at the highest B_T for both L- and H-mode plasmas. Calculation uncertainties in the thermal τ_E are approximately 20%. The quality of the kinetic data at the lowest B_T for L-mode discharges precluded calculating the thermal τ_E at these fields with confidence for these discharges. The global confinement times, normalized to the ITER97L [6] scaling, also show a strong dependence on B_T with average enhancements ranging from 1.3 at 0.3 T to 2 at 0.45 T, and a maximum of 2.7 in the H-mode at the highest B_T. The right panel in Fig. 2 shows that the increase in thermal and global enhancement with B_T is associated with a reduction in the electron transport relative to that of the ions, with χ_e/χ_i decreasing approximately one order of magnitude across this range of B_T.

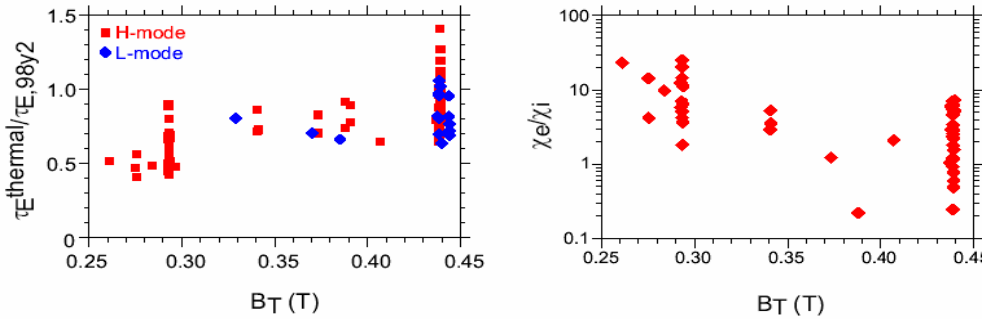

Fig. 2 Thermal confinement enhancement factor relative to conventional R/a values and ratio of χ_e/χ_i as a function of B_T for both L- and H-modes

This strong B_T dependence is borne out in the results from statistical analysis of the full H-mode dataset, with $\tau_E \sim I_p^{0.52}B_T^{0.86}n_e^{0.26}P_{L,th}^{-0.50}$ using the Principal Component Error in Variable technique [7]. In terms of physics variables, the confinement scales as $B_{tot}\tau_{E,th} \sim \rho_*^{-3.44}\beta_{th,tot}^{0.43}\nu_*^{-0.46}$, where the thermal β, $\beta_{th,tot}$, is defined using the total magnetic field, B_{tot}. The normalized confinement scaling is consistent with gyroBohm, and it increases with decreasing collisionality, similar to conventional aspect ratio devices [7]. Unlike at higher R/a, though, NSTX exhibits a positive dependence on β.

It is also seen that there is much scatter in the confinement enhancements at all fields. Several possible sources for the scatter in the confinement enhancement factors for H-mode plasmas at fixed engineering conditions, most notably fixed B_T, have been studied. It was found that neither magnetic activity detected by an array of Mirnov coils over the frequency range from 1 to 200 kHz nor plasma rotation correlated with the scatter of the data. However, it was found that at fixed toroidal field the degradation in confinement enhancement factor was well correlated with an increasing absolute level of fluctuating power $\tilde{n}^2$ in the frequency range from 5 to 20 kHz, as measured by a far-infrared interferometer. This data was obtained from a chord with a tangency radius of 0.85 m, passing through the core region of the plasma in its view. The correlation was weaker when the fluctuation level was normalized by the driving term (i.e., for $\tilde{n}/n$).

Fig. 3 shows two additional sources for the data scatter. Plotted in each figure is the confinement enhancement as a function of ELM amplitude, as determined by the Fourier amplitude of the D_α signal in the frequency range of ELMs for each discharge. Zero ELM amplitude means that the H-mode was ELM-free. The data are sorted differently in each panel; by ELM-type in the left-hand figure and by elongation in the right. ELM severity and type clearly have an effect on confinement, with the average enhancement factors the

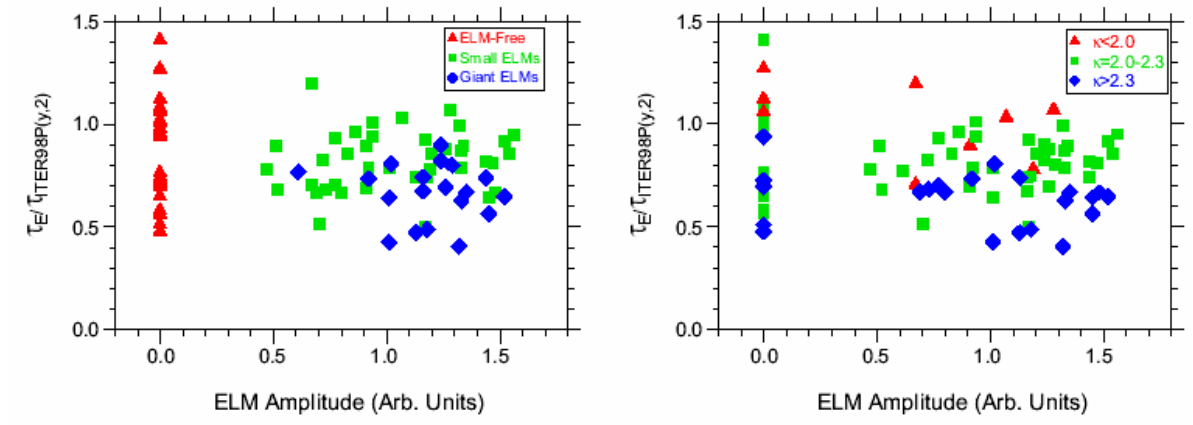

Fig. 3 Confinement enhancement factors vs ELM amplitude sorted by ELM type (left panel) and plasma elongation (right panel)

greatest for ELM-free discharges. Discharges with giant ELMs have the lowest average enhancement factors. The confinement enhancements are also influenced by plasma shape. While the range of elongation for this dataset was narrow, and therefore not included in statistical analyses, the figure on the right shows that confinement was poorer for the higher elongated plasmas. This is most clearly seen for ELM-free discharges; the dependence of ELM-type on κ complicates the interpretation for the subset of discharges which do have ELMs.

Local Transport

The local transport properties of NSTX plasmas have been studied through power balance analysis with the TRANSP code. Inputs to the code include various plasma kinetic profiles (T_e, n_e, T_i, v_{tor}, n_{carbon}), and the beam contribution is determined from a Monte-Carlo guiding center calculation with finite Larmor radius corrections, which are important for the low toroidal field NSTX device. The analysis shows that the electrons are the dominant loss channel in H-mode plasmas [8], with electron thermal diffusivities on average one order of magnitude greater than the ion thermal diffusivity in the plasma core (r/a~0.4). The ion thermal diffusivity is comparable to or is a factor of a few greater than the NCLASS [9]

neoclassical value. Recent neoclassical calculations that incorporate non-local effects using GTC-NEO [10] indicate that the $\chi_{i,NC}$ can be enhanced over that given by NCLASS.

The dominance of electron transport on NSTX makes it an ideal platform on which to study electron confinement physics, and it was found that the electron transport could be improved by manipulating the q-profile through variations in neutral beam timing and plasma current ramp rates early in L-mode discharges. In fact, strong electron transport barriers were seen to develop in discharges for which modeling indicated a magnetic shear reversal, with the electron ITB residing in the region of large negative shear [11]. This reversal of the magnetic shear has been confirmed in recent experiments by measurements of the internal profile of the magnetic field line pitch using the Motional Stark Effect. In these plasmas, the linear growth rates of low-k instabilities (ITG, microtearing) are calculated to be low.

The dominance of electron transport, in addition, allows a study of possible different confinement regions within the plasma. This was accomplished by modeling the rapid response of the electron temperature from large ELM perturbations using a "two-color" soft X-ray spectroscopy. The modeled electron temperature was seen to drop across the profile in response to a large ELM, with two regions with different transport characteristics suggested by the cold pulse propagation. Fig. 4 shows the time-to-peak of the cold pulse as a function of normalized radius along with the T_e profile just prior to the ELM. The rapid propagation of the cold pulse outside of r/a=0.5 suggests a local perturbative heat diffusivity of hundreds of m^2/s in that region, while the perturbative χ_e, χ_e^{PERB}, inside r/a=0.5 is only tens of m^2/s. Power balance calculations indicate $\chi_e^{PB}>\chi_e^{PERB}$ inside r/a=0.5 but $\chi_e^{PB}<<\chi_e^{PERB}$ outside.

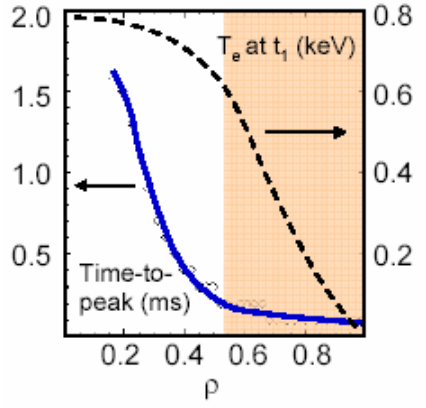

Fig. 4 Time to peak of the ELM cold pulse and T_e profile prior to the ELM

In conclusion, NSTX can provide a view of toroidal confinement physics by operating at low aspect ratio and high β. While some confinement trends are similar to those at conventional aspect ratio, other trends, most notably the strong dependence on B_T and β, are significantly different. The dominance of electron loss in NSTX allows a unique probe into these properties and a determination of the importance of short-wavelength (e.g. ETG mode) induced turbulent transport.

This work is supported by U.S. DOE contract # DE-AC02-76CH03073.

References

[1] Ono, M. et al., Plasma Phys. Controlled Fusion **45** (2003) A335.
[2] Kaye, S.M. et al., to appear in Nucl. Fusion (2005).
[3] Maingi, R et al., Phys. Controlled Fusion **46** (2004) A305.
[4] Sabbagh, S.A. et al., Nucl. Fusion **41** (2001) 1601.
[5] ITER Physics Basis, Nucl. Fusion **39** (199) 2137.
[6] Kaye, S.M. et al., Nucl. Fusion **37** (1997) 1303.
[7] Cordey, J.G. et al., to appear in Nucl. Fusion (2005).
[8] LeBlanc, B.P. et al., Nucl. Fusion **44** (2004) 513.
[9] Houlberg, W. et al., Phys. Plasmas **4** (1997) 3230.
[10] Wang, W.X. et al., Comput. Phys. Commun. **164** (2004) 178.
[11] Stutman, D. et al., to appear in Nucl. Fusion (2005).